Wind and Structures, Vol. 2, No. 3 (1999) 151-171
DOI: http://dx.doi.org/10.12989/was.1999.2.3.151

A linear model for structures with Tuned Mass Dampers

Francesco Ricciardelli†

Department of Mechanics and Materials, University of Reggio Calabria, Via Graziella, Feo di Vito, Reggio Calabria, Italy

Abstract. In its 90 years of life, the Tuned Mass Damper have found application in many fields of engineering as a vibration reducing device. The evolution of the theory of TMDs is briefly outlined in the paper. A generalised mathematical linear model for the analysis of the response of line-like structures with TMDs is presented. The system matrices of the system including the TMDs are written in the state space as a function of the mean wind speed. The stability of the system can be analysed and the Power Spectral Density Function of any response parameter calculated, taking into account an arbitrary number of modes of vibration as well as an arbitrary number of TMDs, for any given PSDF of the excitation. The procedure can be used to optimise the number, position and mechanical properties of the damping devices, with respect to any response parameter. Due to the stationarity of the excitation, the method is well suited to structures subjected to the wind action. In particular the procedure allows the calculation of the onset galloping wind speed and the response to buffeting, and a linearisation of the aeroelastic behaviour allows its use also for the evaluation of the response to vortex shedding. Finally three examples illustrate the suggested procedure.

Key words: wind excited response; passive control; Tuned Mass Dampers.

1. Introduction

1.1. The Fixed Points Theory

Close to its centenary the Tuned Mass Damper still proves to be a quite effective means to mitigate the response of dynamic systems, and though the behaviour is almost intuitive, the wide range of its applications makes it the subject of a large number of papers.

The first application of a TMD dates back 1909, when Frahm used a U shaped water column to reduce the rolling of ships.

The first theoretical study on the behaviour of systems with TMDs can be found in Ormondroyd and Den Hartog (1928) and Den Hartog (1940) with additions appeared in Brock (1946), while the complete theory can be found in the 1956 edition of Den Hartog's book. An undamped linear SDOF system with either an undamped or a damped linear TMD, and subjected to harmonic excitation was considered. Effective in reducing the response at resonance, the undamped TMD has to be discarded because the amplitude of vibration of the

† Assistant Professor

secondary system is quite large and because the undamped resonance is shifted in frequency but not eliminated. The behaviour of a system with either a TMD with viscous damping or a Lanchester damper was studied through the Fixed Points Theory (FPT). It was observed that the response curves of the primary system for different values of the damper's damping all intersect at two points. The optimum tuning is chosen so that the two fixed points have equal ordinates, while the optimum damper's damping is chosen to give the response curve a horizontal tangent through one of the fixed points. This leads to approximately minimise the maximum amplitude of vibration of the primary system with varying frequency of excitation.

The systems considered by Den Hartog are rather simplistic but the approach quite elegant, and the theory provides a clear understanding of the changes brought to the system by the addition of a TMD. A large amount of papers followed dealing with more realistic systems and analysing many different aspects of the behaviour of TMDs.

The FPT was extended to systems having complex stiffness (Snowdon 1959), and to systems with a damped and an undamped TMD in parallel (Srinivasan 1969), but is unable to account for the damping of the primary system. However, for a lightly damped system with a small added mass, the optimum damper's damping is little affected by the damping of the primary system, so it was suggested (Bapat and Kumaraswamy 1979) that the optimisation criterion of the FPT be used also for a lightly damped primary system. A poor estimate of the response of the primary system, however, would result from neglecting its damping.

A quite different approach to the analysis of systems with TMDs was presented by Falcon *et al.* (1967), based on a graphical procedure. More recently a damped SDOF system subjected to sinusoidal base acceleration or displacement was numerically analysed by Tsai and Lin (1993), and interpolating expressions for the TMD optimum parameters were given.

1.2. The application to continuous systems

The study of the effectiveness of TMDs through the FPT led to significant results. However, practical systems are in general more complicated, and two questions arise: first, to what extent a SDOF system well describes the behaviour of the primary system; second, how to establish a correspondence between the real system and the equivalent SDOF system.

The longitudinal oscillation of a bar was considered by Neubert (1964), while the lateral oscillation of a beam was considered by Snowdon (1966) and Jacquot (1978). In Warburton and Ayorinde (1980) and Ayorinde and Warburton (1980), the approach by Jacquot was generalised to a wider range of structures: beams, rods, plates and shells.

1.3. The response to a non-sinusoidal excitation. TMDs for civil engineering applications

To the author's knowledge, the first paper to consider the behaviour of a system subjected to a non-sinusoidal excitation is that by Curtis and Boykin (1961), in which the effect of a TMD attached to a damped SDOF system subjected to white noise was numerically investigated. Again in the case of a white noise input, Crandall and Mark (1963) found expressions for the variance of the response of the primary and auxiliary systems, and Jacquot and Hoppe (1973) presented an algebraic equation whose solution gives the optimum damper's damping for a given value of the tuning and of the primary system parameters.

The first explicit application of the TMD theory to civil engineering problems appeared in Gupta and Chandrasekaren (1969). The equations of motion of a SDOF system with a bi-linear hysterisis and viscous damping to which a number of TMDs are attached were numerically integrated for a seismic input. The use of a number of TMDs facilitate control of a range of frequencies, and the idea was again considered in many papers that followed.

Following the approach by Crandall and Mark, Wirsching and Campbell (1974) numerically studied the response of multi-storey buildings subjected to ground motion, and McNamara (1977) investigated the performance of TMDs in reducing the alongwind response of tall buildings. The latter introduced the concept of equivalent damping, i.e., the damping that would lead the plain primary system to the same response that it has with a given TMD. Only for the case in which the primary system is undamped, approximate expressions for the optimum TMD's parameters were given by Luft (1979) and Ayorinde and Warburton (1980).

Although the use of a stationary Gaussian white noise input to study the resonant response to the atmospheric turbulence is almost accurate, it is clear that this can lead to significant errors in the case of a ground motion excitation. This point was dealt with by Kaynia *et al.* (1981), who integrated the equation of motion of a SDOF system with and without a TMD for a population of earthquakes, pointing out a generally poor seismic performance of the TMD. The findings were also confirmed by Sladek and Klingner (1983), who numerically evaluated the response of a 25-story building to the N-S component of the 1940 El Centro earthquake.

The use of a TMD to reduce the galloping behaviour of a structure was first dealt with by Fujino *et al.* (1985), using the method by Krylov and Bogoliubov. Abdel-Rohman (1994) applied the method of multiple scales to calculate the galloping amplitude of a prismatic structure. However, in the case in which a TMD is attached to the structure, the solution of the equations gets more involved, and only the onset wind speed is obtained.

A more realistic buffeting and vortex shedding-induced excitation was considered by Xu *et al.* (1992), who presented a semi-analytical procedure for the calculation of the response of tall buildings. The PSDF of the excitation has in this case to be obtained through wind tunnel measurements. A comparison between the predicted response and that resulting from wind tunnel tests on a model provided with a TMD showed a good agreement in the case of a forced motion (both alongwind and acrosswind), but also showed an overestimation of the self-excited response (acrosswind response in the lock-in range).

In the last two decades, quite a large number of papers appeared dealing with the use of tuned masses to reduce the resonant response of structures, and new control strategies were introduced, such as Tuned Sloshing Dampers (TSD), Multiple Tuned Mass Dampers (MTMD), Semi-Active and Active Tuned Mass dampers (SATMD, ATMD). Samali *et al.* (1985), for example, considered the use of an ATMD for the mitigation of the buffeting response of a tall building, showing its higher efficiency for the reduction of the accelerations.

1.4. Motivation of the research

From the analysis of the referenced papers and of the many others that can be found in the literature, the following considerations can be drawn:

a. the primary system is quite often modelled as a SDOF system; very seldom higher modes are considered and even less often coupled modes;

b. the optimisation of the TMD parameters is always carried out minimising the displacement of the primary system; in very few cases the response of the auxiliary system is considered;
c. the use of more TMDs in Civil Engineering applications is very seldom considered, and no criteria can be found for the choice of the number, position and properties of the TMDs;
d. the excitation is almost always modelled as either a sinusoidal or a white-noise input.

In the remaining part of the paper, a generalised linear model for the analysis of the stationary response of line-like structures with TMDs is presented. The model can account for any number of modes of vibration as well as for any number of TMDs, and can calculate the onset galloping wind speed and any parameter of the structural response under a specified excitation. The drawback of such a general approach is that it requires to numerically evaluate the response and is unable to provide expressions for the optimum TMD parameters.

In section 2, the displacement of a line-like structure with TMDs is first expressed in a general form, then in the case in which only a limited number of modes of vibration are considered. For the latter case, the equation of motion is written, including the aerodynamic damping and stiffness terms. The equation of motion is then rewritten in section 3 using a state-space approach, and the expression of the PSDF of the response is given as a function of the system matrices and of the PSDF of the excitation. In section 4, the aerodynamic damping and stiffness matrices are written, as well as the PSDF of the excitation due to buffeting and vortex shedding. Three examples are presented in section 5 to illustrate the procedure.

2. A mathematical model for line-like structures with TMDs

2.1. Distributed-parameters systems

The deformed shape of a line-like structure can be described by a three component vector function of the abscissa z, representing the components of the in-plane rigid body motion of the cross-sections. Consistently each TMD is modelled as an in-plane two degree of freedom spring-dashpot system connected to the structure at the location z_k (Fig. 1).

The displacement σ of the system is given by the pair:

$$\sigma = (s(z), \delta) \tag{1}$$

where $s(z) = [x(z)\ y(z)\ \vartheta(z)]^T$ is the displacement of the structure, where $\delta = [\delta_1 \cdots \delta_k \cdots \delta_m]^T$ is the array of the absolute displacements of the m TMDs. The displacement of the k-th TMD is the two component vector $\delta_k = [\delta_{kx}\ \delta_{ky}]^T$.

To study the motion of the system, all the above quantities are considered continuous functions of time in $(0, +\infty)$.

2.2. Discrete model

If n structural modes of vibration are considered, the system described by Eq. (1) reduces to a finite degree of freedom system. The displacement of the discrete system can be written as:

$$\sigma = \sum_{i=1}^{p} \sigma_i \cdot \eta_i(t) \tag{2}$$

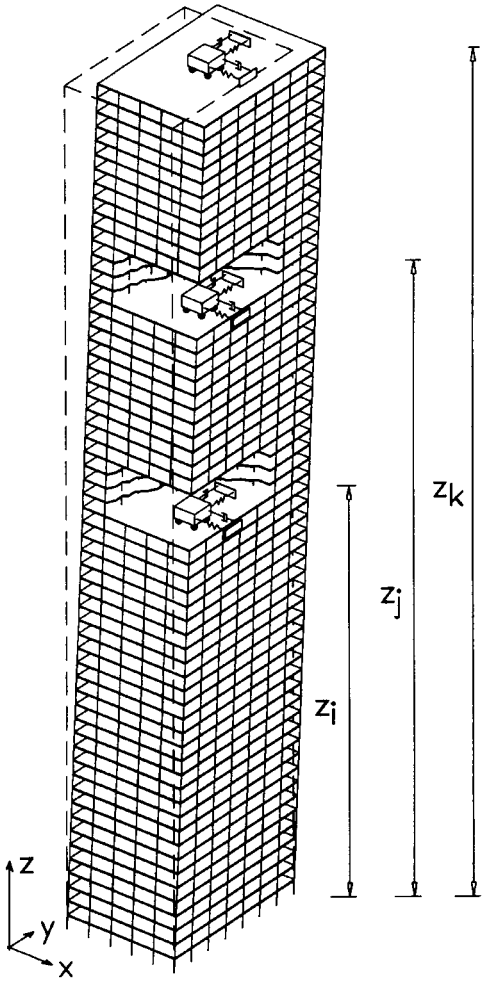

Fig. 1 High rise building with three Tuned Mass Dampers

η_i and σ_i being the i-th generalised co-ordinate and shape function respectively, with:

$$\sigma_i = (\mu_i(z), \mathbf{0}) \quad i \in \{1, \cdots n\} \tag{3a}$$

$$\sigma_i = (\mathbf{0}(z), v_{i-n}) \quad i \in \{n+1, \cdots p\} \tag{3b}$$

where $p = n+2\times m$.

In Eqs. (3), $\mu_i(z) = \{\mu_{ix}(z)\ \mu_{iy}(z)\ \mu_{i\vartheta}(z)\}^T$ is the i-th natural mode of vibration of the structure without TMDs, $\mathbf{0}$ and $\mathbf{0}(z)$ are the $2\times m$-dimensional array of zeroes and the three component nil function in $[0, L]$ respectively, and v_j is the array characterising the j-th component of the displacement of the TMDs, i.e., a $2\times m$-dimensional array having unitary j-th component and zeroes elsewhere. It appears that the first n shape functions represent the considered structural modes of vibrations, while each of the remaining represents one component of the displacement of one of the TMDs.

2.3. Equation of motion

The equation of motion for the discrete system described by Eq. (2) takes the form:

$$[\mathbf{M}]\ddot{\eta}(t)+[\mathbf{C}^*]\dot{\eta}(t)+[\mathbf{K}^*]\eta(t)=f(t) \tag{4}$$

where η is the array of the generalised co-ordinates and f is a p-component vector, only the first n being non-zero for the excitation acts only on the primary system.

The mass matrix in Eq. (4) is the $p\times p$ diagonal matrix:

$$[\mathbf{M}]=\begin{bmatrix} m_1 & & & \\ & \ddots & & \\ & & m_n & \\ \hline & & & \mathbf{M}_1 \\ & & & & \ddots \\ & & & & & \mathbf{M}_m \end{bmatrix} \tag{5}$$

where m_i is the i-th modal mass of the structure without TMDs:

$$m_i=\int_0^L \mu_i^{\mathrm{T}}(z)[\mathbf{M}(z)]\mu_i(z)\,dz \tag{6}$$

with:

$$[\mathbf{M}(z)]=\begin{bmatrix} m(z) & & \\ & m(z) & \\ & & I(z) \end{bmatrix} \tag{7}$$

$m(z)$ and $I(z)$ being the mass and mass moment of inertia per unit length of the structure, and where $\mathbf{M}_i$ is the mass matrix of the i-th TMD:

$$[\mathbf{M}_i]=\begin{bmatrix} m_i^d & \\ & m_i^d \end{bmatrix} \tag{8}$$

m_i^d being the mass of the i-th TMD.

The asterisk to the total damping and stiffness matrices in Eq. (4) indicates that the two matrices are, in general, sum of structural and aerodynamic components. The structural components of the damping and stiffness matrices can be written as:

$$[\mathbf{C}]=\begin{bmatrix} c_{1,1}+\mathbf{c}_{1,1}^d & \cdots & c_{1,n}+\mathbf{c}_{1,n}^d & \mathbf{c}_{1,n+1}^d & \cdots & \mathbf{c}_{1,n+m}^d \\ \vdots & & \vdots & \vdots & & \\ c_{n,1}+\mathbf{c}_{n,1}^d & \cdots & c_{n,n}+\mathbf{c}_{n,n}^d & \mathbf{c}_{n,n+1}^d & \cdots & \mathbf{c}_{n,n+m}^d \\ \hline \mathbf{c}_{n+1,1}^d & \cdots & \mathbf{c}_{n+1,n}^d & \mathbf{C}_1^d & & \\ \vdots & & \vdots & & \ddots & \\ \mathbf{c}_{n+m,1}^d & \cdots & \mathbf{c}_{n+m,n}^d & & & \mathbf{C}_m^d \end{bmatrix} \tag{9a}$$

$$[\mathbf{K}] = \left[\begin{array}{ccc:ccc} k_1+k_{1,1}^d & \cdots & k_{1,n}^d & \mathbf{k}_{1,n+1}^d & \cdots & \mathbf{k}_{1,n+m}^d \\ \vdots & & \vdots & \vdots & & \\ k_{n,1}^d & \cdots & k_n+k_{n,n}^d & \mathbf{k}_{n,n+1}^d & \cdots & \mathbf{k}_{n,n+m}^d \\ \hdashline \mathbf{k}_{n+1,1}^d & \cdots & \mathbf{k}_{n+1,n}^d & \mathbf{K}_1^d & & \\ \vdots & & \vdots & & \ddots & \\ \mathbf{k}_{n+m,1}^d & \cdots & \mathbf{k}_{n+m,n}^d & & & \mathbf{K}_m^d \end{array}\right] \tag{9b}$$

where the *d* superscript indicates the terms related to the presence of the TMDs.

Neglecting the cross terms of the structural damping, the structural terms in Eqs. (9) are $c_{ii} = 4\pi\xi_i f_i m_i$ and $k_i = (2\pi f_i)^2 m_i$, f_i and ξ_i being the *i*-th natural frequency and damping ratio of the structure without TMDs respectively.

In Eqs. (9), the terms related to the TMDs' properties have the following expressions:

$$c_{i,j}^d = \sum_{k=1}^{m} \mu_i^{\mathrm{T}}(z_k)\,[\mathbf{C}_k']\,\mu_j(z_k) \tag{10a}$$

$$k_{i,j}^d = \sum_{k=1}^{m} \mu_i^{\mathrm{T}}(z_k)\,[\mathbf{K}_k']\,\mu_j(z_k) \tag{10b}$$

$$\mathbf{c}_{i,j}^d = -\,\mu_i^{\mathrm{T}}(z_k)\,[\mathbf{C}_k']\,[\mathbf{P}] \qquad \text{for } i \le n,\quad j=n+k \tag{11a}$$

$$\mathbf{k}_{i,j}^d = -\,\mu_i^{\mathrm{T}}(z_k)\,[\mathbf{K}_k']\,[\mathbf{P}] \tag{11b}$$

$$\mathbf{c}_{i,j}^d = -\,[\mathbf{P}]^{\mathrm{T}}\,[\mathbf{C}_j']\,\mu_j(z_j) \qquad \text{for } i > n,\quad j \le n \tag{12a}$$

$$\mathbf{k}_{i,j}^d = -\,[\mathbf{P}]^{\mathrm{T}}\,[\mathbf{K}_j']\,\mu_j(z_j) \tag{12b}$$

$$\mathbf{C}_k^d = [\mathbf{P}]^T\,[\mathbf{C}_k']\,[\mathbf{P}] \tag{13a}$$

$$\mathbf{K}_k^d = [\mathbf{P}]^T\,[\mathbf{K}_k']\,[\mathbf{P}] \tag{13b}$$

where:

$$[\mathbf{C}_k'] = \begin{bmatrix} c_{k,x} & 0 & c_{k,x}\,d_{k,y} \\ 0 & c_{k,y} & -\,c_{k,y}\,d_{k,x} \\ c_{k,x}\,d_{k,y} & -\,c_{k,y}\,d_{k,x} & c_{k,x}\,d_{k,y}^2 + c_{k,y}\,d_{k,x}^2 \end{bmatrix} \tag{14a}$$

$$[\mathbf{K}_k'] = \begin{bmatrix} k_{k,x} & 0 & k_{k,x}\,d_{k,y} \\ 0 & k_{k,y} & -\,k_{k,y}\,d_{k,x} \\ k_{k,x}\,d_{k,y} & -\,k_{k,y}\,d_{k,x} & k_{k,x}\,d_{k,y}^2 + k_{k,y}\,d_{k,x}^2 \end{bmatrix} \tag{14b}$$

$$[\mathbf{P}] = \begin{bmatrix} 1 & 0 \\ 0 & 1 \\ 0 & 0 \end{bmatrix} \tag{14c}$$

$c_{k,x}$, $c_{k,y}$, $k_{k,x}$ and $k_{k,y}$ being the damping and stiffness properties of the k-th TMD, and $d_{k,x}$ and $d_{k,y}$ being its eccentricities with respect to the centre of gravity of the cross-section.

The TMD stiffness and damping are usually expressed through the dampers' frequency and damping ratio as $c_{k,x} = 4\pi\xi_{k,x} f_{k,x} m_k$, $c_{k,y} = 4\pi\xi_{k,y} f_{k,y} m_k$, $k_{k,x} = (2\pi f_{k,x})^2 m_k$ and $k_{k,y} = (2\pi f_{k,y})^2 m_k$.

3. Solution of the equation of motion

Any response parameter linearly related to the state of the system and to the exciting force can be calculated from Eq. (4) using a state-space approach. Defining the state vector of the system as $z = [\eta \ \dot{\eta}]^T$, Eq. (4) can be rewritten as

$$\dot{z}(t) = [\mathbf{A}^*] z(t) + [\mathbf{B}] f(t) \tag{15}$$

where:

$$[\mathbf{A}^*] = \begin{bmatrix} \mathbf{0}_p & \mathbf{I}_p \\ -\mathbf{M}^{-1}\mathbf{K}^* & -\mathbf{M}^{-1}\mathbf{C}^* \end{bmatrix} \tag{16a}$$

$$[\mathbf{B}] = \begin{bmatrix} \mathbf{0}_n \\ \mathbf{0}_{2m} \\ 1/m_1 \\ \ddots \\ 1/m_n \\ \mathbf{0}_{2m} \end{bmatrix} \tag{16b}$$

In Eq. (16a), $\mathbf{0}_p$ and $\mathbf{I}_p$ are the p-th order zero and unity matrices respectively, while in Eq. (16b), $\mathbf{0}_n$ and $\mathbf{0}_{2m}$ are the n-th order and $2m$-th order zero matrices.

The q-dimensional response vector $\boldsymbol{y}$ is a linear combination of the state of the system and of the excitation:

$$\boldsymbol{y}(t) = [\mathbf{E}] z(t) + [\mathbf{D}] f(t) \tag{17}$$

Using this approach, the aeroelastic stability of the system can be checked by studying the signs of the real parts of the eigenvalues of the $2p \times 2p$ state matrix $[\mathbf{A}^*]$ with varying wind velocity. A stable behaviour occurs only for wind velocities for which the real parts of all the eigenvalues are negative.

Eqs. (15) and (17) can be used to evaluate the PSDM of the response if that of the excitation is known. It can be shown with simple algebra that (Occhiuzzi and Ricciardelli 1996):

$$[\mathbf{S}_{yy}(f)] = [\mathbf{G}^*(f)] [\mathbf{S}_{ff}(f)] \overline{[\mathbf{G}^*(f)]}^T \tag{18}$$

where $[\mathbf{S}_{ff}(f)]$ is the $n \times n$ PSDM of the non zero components of the excitation, and where:

$$[\mathbf{G}^*(f)] = [\mathbf{E}] [i 2\pi f \, \mathbf{I} - \mathbf{A}^*]^{-1} [\mathbf{B}] + [\mathbf{D}] \tag{19}$$

is the transfer function directly associated with the Fourier transform of the input $\mathbf{F}(f)$ and

the Fourier transform of the output $\mathbf{Y}(f)$. $[\mathbf{G}^*(f)]$ is a $q \times n$ matrix fully representative of the system properties, and when the output is the modal displacement, it coincides with the well-known complex frequency response function or mechanical admittance function.

In most cases only the diagonal terms of the PSDM of the response are of interest, that can be expressed as:

$$\mathbf{S}_{yy}(k) = \sum_j \sum_i \mathbf{S}_{ji}\, \mathbf{G}_{kj}\, \bar{\mathbf{G}}_{ki} \tag{20}$$

where the dependency on the frequency has been omitted for brevity.

In this paper, the structural response (Eq. (17)) is calculated by superimposing a limited number of modes, using the traditional *mode-displacement method* (Borino and Muscolino 1986). A better estimate of the background response can be obtained by accounting for the contribution of part of the neglected modes through the *mode-acceleration method* or through the *dynamic correction method*. This, however, would not improve the analysis of the performance of the TMDs, since it will affect only the background response, which is not controlled by the TMDs.

4. Response of wind action

The analysis of the response to wind action is carried out assuming that the loading process can be separated into a mean and a nil-mean fluctuating action. The fluctuating action is considered as a random, Gaussian, stationary process. The mean response is not affected by the presence of the TMDs and therefore is not dealt with herein.

4.1. Aerodynamic damping and stiffness matrices

The aeroelastic damping and stiffness matrices in Eq. (4) can be written as:

$$[\boldsymbol{C}^a] = \left[\begin{array}{ccc:ccc} c^a_{1,1} & \cdots & c^a_{1,n} & 0 & \cdots & 0 \\ \vdots & & \vdots & \vdots & & \vdots \\ c^a_{n,1} & \cdots & c^a_{n,n} & 0 & \cdots & 0 \\ \hdashline 0 & \cdots & 0 & 0 & \cdots & 0 \\ \vdots & & \vdots & \vdots & & \vdots \\ 0 & \cdots & 0 & 0 & \cdots & 0 \end{array}\right] \tag{21a}$$

$$[\boldsymbol{K}^a] = \left[\begin{array}{ccc:ccc} k^a_{1,1} & \cdots & k^a_{1,n} & 0 & \cdots & 0 \\ \vdots & & \vdots & \vdots & & \vdots \\ k^a_{n,1} & \cdots & k^a_{n,n} & 0 & \cdots & 0 \\ \hdashline 0 & \cdots & 0 & 0 & \cdots & 0 \\ \vdots & & \vdots & \vdots & & \vdots \\ 0 & \cdots & 0 & 0 & \cdots & 0 \end{array}\right] \tag{21b}$$

in which only the upper left $n \times n$ submatrix is non-zero since the aerodynamic forces act only on the main structure. The terms in Eqs. (21) can be calculated as:

$$c^a_{i,j} = \int_0^L \mu_i^{\mathrm{T}}(z)\,[\,\mathbf{C}^a(z)\,]\,\mu_i(z)\,dz \tag{22a}$$

$$k^a_{i,j} = \int_0^L \mu_i^{\mathrm{T}}(z)\,[\,\mathbf{K}^a(z)\,]\,\mu_i(z)\,dz \tag{22b}$$

The local aerodynamic damping and stiffness matrices $[\mathbf{C}^a(z)]$ and $[\mathbf{K}^a(z)]$ appearing in Eqs. (22) have the following expressions (Solari 1994):

$$[\mathbf{C}^a(z)] = \frac{1}{2}\rho U(z)\,b(z) \begin{bmatrix} 2\bar{C}_D & \bar{C}'_D - \bar{C}_L & R_0(z)(\bar{C}'_D - \bar{C}_L) \\ 2\bar{C}_L & \bar{C}_D + \bar{C}'_L & R_0(z)(\bar{C}_D + \bar{C}'_L) \\ 2b(z)\bar{C}_M & b(z)\,\bar{C}'_M & b(z)R_0(z)\bar{C}'_M \end{bmatrix} \tag{23a}$$

$$[\mathbf{K}^a(z)] = \frac{1}{2}\rho U^2(z)\,b(z) \begin{bmatrix} 0 & 0 & \bar{C}'_D \\ 0 & 0 & \bar{C}'_L \\ 0 & 0 & b(z)\bar{C}'_M \end{bmatrix} \tag{23b}$$

ρ being the air density, U the mean wind speed, b a characteristic dimension of the cross-section, $\bar{C}_D$, $\bar{C}_L$ and $\bar{C}_M$ the mean aerodynamic coefficients of the cross-section, R_0 a characteristic dimension of elongated cross-sections, and where the prime indicates the differentiation with respect to the angle of attack. If the shape of the cross-section varies along the structure, the aerodynamic coefficients in Eqs. (23) would have to be considered as functions of z.

4.2. Exciting force

The power spectral density matrix of the excitation is:

$$[\mathbf{S}_{\mathrm{ff}}(f)] = \begin{bmatrix} \mathbf{S}_{f_1 f_1}(f) & \cdots & \mathbf{S}_{f_1 f_n}(f) \\ \vdots & & \vdots \\ \mathbf{S}_{f_n f_1}(f) & \cdots & \mathbf{S}_{f_n f_n}(f) \end{bmatrix} \tag{24}$$

where each term is the sum of two components due to the longitudinal and transverse turbulence respectively, and a component due to vortex shedding.

The components due to turbulence are (Ricciardelli 1996):

$$S^u_{f_i f_j}(f) = \rho^2 \int_0^L U(z_2)b(z_2) \int_0^L U(z_1)b(z_1)\,\mathrm{C}_{iju}(z_1, z_2)\,S_{uu}(z_1, z_2, f)\,dz_1\,dz_2 \tag{25a}$$

$$S^v_{f_i f_j}(f) = \frac{1}{4}\rho^2 \int_0^L U(z_2)b(z_2) \int_0^L U(z_1)b(z_1)\,\mathrm{C}_{ijv}(z_1, z_2)\,S_{vv}(z_1, z_2, f)\,dz_1\,dz_2 \tag{25b}$$

with:

$$C_{iju}(z_1, z_2) = \mu_i^T(z_1) \begin{bmatrix} \bar{C}_D^2 & \bar{C}_D \bar{C}_L & b(z_2) \bar{C}_D \bar{C}_M \\ \bar{C}_L \bar{C}_D & \bar{C}_L^2 & b(z_2) \bar{C}_L \bar{C}_M \\ b(z_1) \bar{C}_D \bar{C}_M & b(z_1) \bar{C}_D \bar{C}_M & b(z_1) b(z_2) \bar{C}_M^2 \end{bmatrix} \mu_j(z_2) \qquad (26a)$$

$$C_{ijv}(z_1, z_2) =$$

$$\mu_i^T(z_1) \begin{bmatrix} \left(\bar{C}_D' - \bar{C}_L\right)^2 & \left(\bar{C}_D' - \bar{C}_L\right)\left(\bar{C}_D + \bar{C}_L'\right) & b(z_2)\left(\bar{C}_D' - \bar{C}_L\right)\bar{C}_M' \\ \left(\bar{C}_D' - \bar{C}_D\right)\left(\bar{C}_D + \bar{C}_L'\right) & \left(\bar{C}_D + \bar{C}_L'\right)^2 & b(z_2)\left(\bar{C}_D + \bar{C}_L'\right)\bar{C}_M' \\ b(z_1)\left(\bar{C}_D' - \bar{C}_L\right)\bar{C}_M' & b(z_1)\left(\bar{C}_D + \bar{C}_L'\right)\bar{C}_M' & b(z_1) b(z_2) \bar{C}_M'^2 \end{bmatrix} \mu_j(z_2) \qquad (26b)$$

and where the cross-spectral density functions of the components of turbulence S_{uu} and S_{vv} are usually expressed as the product of a local spectrum and a coherence function.

The component of the excitation due to vortex shedding can be expressed in a form similar to that of Eqs. (25), by introducing the fluctuating wake aerodynamic coefficients. Knowledge on these coefficients can be gained from the results of wind tunnel tests, separating the portion of the fluctuating forces due to vortex shedding from those due to buffeting.

An alternative approach is that suggested in Ricciardelli (1996), based on the direct calculation of the total mean and fluctuating forces from wind tunnel pressure measurements.

4.3. Response to vortex shedding in the lock-in range

One of the most common applications of TMDs in civil engineering is that aimed at the reduction of the vortex shedding induced response of chimneys in the lock-in range. A linear approach would in that case not lead to accurate results due to strong non-linearity of the system arising from its aeroelastic behaviour. However, the linear procedure can still be used under certain conditions.

Following the approach by Vickery (1993), the shedding induced response of a slender structure of circular cross-section can be calculated considering the forces acting on the stationary body and accounting for the non-linear behaviour through an aerodynamic damping term, which is non-linearly dependent of the wind speed and the rms displacement. The aerodynamic damping force per unit length is:

$$F_a(z,t) = -4\pi\rho b^2(z) f_1 \left\{ \frac{k(z)}{10} - \frac{k^2(z)}{1+6I_u(z)} \exp\left[-\left(\frac{6(k(z)-1)}{1+6I_u(z)} \right)^2 \right] \right\} \times \left[1 - \left(\frac{\tilde{y}(z)}{\alpha b(z)} \right)^2 \right] \cdot \dot{y}(z,t) = c^s(z) \cdot \dot{y}(z,t) \quad (27)$$

where k is the ratio of the wind speed to its critical value, I_u is the longitudinal intensity of turbulence and αb is the limiting amplitude ($\alpha \cong 0.4$).

Assuming that the TMD limits the motion of the chimney to small amplitudes, i.e., $\tilde{y} << \alpha b$, one can neglect the term $(\tilde{y}/\alpha b)^2$ in Eq. (27) and directly calculate the aerodynamic damping in the first acrosswind mode as a function of the reference wind speed:

$$c^a_{1,1} = \int_0^L c^s(z) \mu^2_{1y}(z)\, dz \quad (28)$$

where $c^s(z)$ is the shedding damping coefficient defined in Eq. (27).

5. Examples

The procedure presented in the previous paragraphs was implemented in a MATLAB routine. Three examples of application follow, the first and the third dealing with the buffeting response and galloping behaviour of two tall buildings respectively, and the second with the vortex shedding induced response of a chimney.

5.1. Example 1

The alongwind buffeting response of a 120 m tall rectangular building was considered. The width of the building is 30 m and the mass 3×10^5 kg/m. A drag coefficient of 1.4 was used in the calculations. The first 2 modes were taken into account. The natural frequencies and damping ratios are : $f_1 = 0.35$ Hz, $f_2 = 1.60$ Hz and $\xi_1 = 0.008$, $\xi_2 = 0.012$.

A power law with $\alpha = 0.25$ was used for the mean wind speed profile with a reference velocity $U_{10} = 30$ m/s. The local atmospheric turbulence was described through the Davenport spectrum with a uniform intensity of turbulence $I_u = 0.10$, and its vertical coherence with an exponential law with a decay coefficient $c_z = 8$.

Seven cases were considered: the plain structure and six cases with a TMD placed at the roof level. In all the cases the TMD has a mass of 1% of the first modal mass of the building. Table 1 shows the rms tip displacement and base shear and moment of the building and the rms relative displacement of the TMD.

The second mode contributes less than 0.2% to the displacement of the plain structure, and for this reason was neglected in the calculations. This is the classical case of a SDOF system with a TMD attached, often dealt with in the literature, and the results obtained can be compared to those obtained with different approaches by other authors.

Table 1 Example 1 : rms tip displacement and TMD relative displacement

		plain	case 1	case 2	case 3	case 4	case 5	case 6
ξ_{TMD}		-	0.05	0.05	0.05	0.03	0.10	0.15
Ω		-	1.00	0.99	0.96	0,96	0.96	0.96
rms tip displacement	[cm]	1.89	1.05	1.03	1.02	1.10	0.99	1.01
rms TMD displacement	[cm]	-	3.40	3.44	3.50	4.37	2.52	2.03

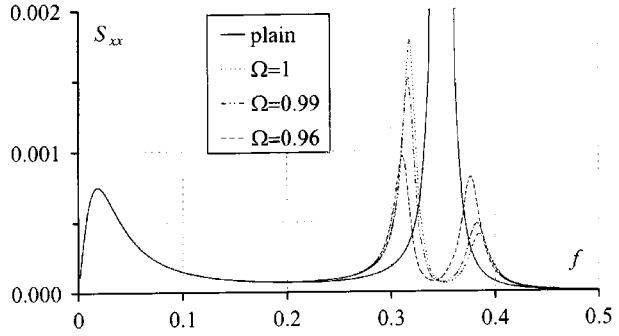

Fig. 2 Example 1 : PSDF of the tip displacement for $\xi_{TMD} = 0.05$

Three tuning ratios were considered of $\Omega = 1.00$ (case 1), $\Omega = 0.99$ (case 2) and $\Omega = 0.96$ (case 3), with a damper's damping of $\xi_{TMD} = 0.05$ (the optimum damping value after McNamara, i.e., using a white noise input). Following the procedure by McNamara, the optimum tuning would be $\Omega = 0.99$; however it can be seen the optimum tuning is $\Omega = 0.96$. A lower optimum tuning in the case in which a real turbulence spectrum is used was already found in Xu *et al.* (1992b), and the reason for that has to be seen in the shape of the turbulence spectrum, having higher values at the low frequencies. Referring to Fig. 2, in fact, it can be seen how the first peak tends to be amplified by the low frequency turbulence, and thus it is necessary to reduce the TMD's frequency in order to balance the two peaks.

The maximum global reduction in the rms tip displacement that can be achieved with a damper's damping of 0.05 is 46%. The effectiveness of the TMD can be seen looking at the background and resonant portions of the rms response; for the plain structure the background and resonant rms tip displacements are 0.70 cm and 1.76 cm respectively, while for case 3 the resonant rms tip displacements decreases to 0.75 cm.

For a tuning of $\Omega = 0.96$, three more values of the damper's damping were considered: $\xi_{TMD} = 0.03$ (case 4), $\xi_{TMD} = 0.10$ (case 5) and $\xi_{TMD} = 0.15$ (case 6) respectively. In Fig. 3 the power spectral density functions of the tip displacements are plotted for a tuning of $\Omega = 0.96$, showing a better performance of the TMD can be achieved by increasing the damper's damping beyond the optimum value given by McNamara. Case 5 leads to a resonant part of the rms tip displacement of 0.70 cm.

Generally the TMD's response proves to be little influenced by the tuning, but strongly influenced by the damper's damping (Table 1).

A modified version of the building, having a second natural frequency of 0.7 Hz, was then considered. In this case the damping ratio in the first and second mode are 0.012 and 0.008

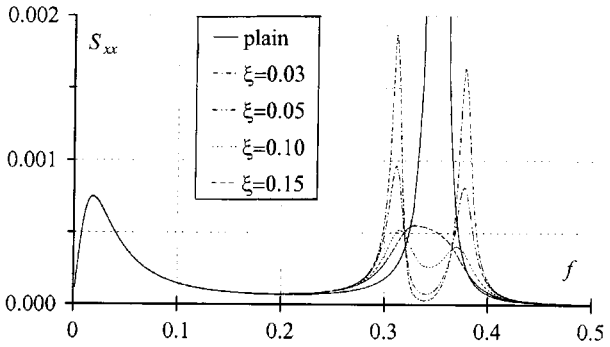

Fig. 3 Example 1 : PSDF of the tip displacement for $\Omega = 0.96$

Table 2 Example 1 : Fluctuating tip displacements and accelerations of the modified building

			plain	case 1a	case 2a	case 3a	case 4a
	ξ_{TMD1}		-	0.05	0.05	0.05	0.09
	Ω_1		-	1.00	0.96	0.96	0.96
	ξ_{TMD2}		-	-	-	0.05	0.09
	Ω_2		-	-	-	0.96	0.96
tip displacement	var-background	[cm^2]	0.434	0.436	0.436	0.436	0.436
	var-1st mode	[cm^2]	2.08	0.570	0.526	0.524	0.460
	var-2nd mode	[cm^2]	0.055	0.046	0.047	0.013	0.012
	rms	[cm]	1.60	1.04	1.00	0.99	0.95
tip acceleration	var-1st mode	[$cm^2 \cdot s^{-4}$]	9.92	2.48	2.40	2.38	2.08
	var-2nd mode	[$cm^2 \cdot s^{-4}$]	1.02	0.862	0.874	0.208	0.197
	rms	[$cm \cdot s^{-2}$]	3.31	1.83	1.81	1.60	1.51

respectively. For the plain structure, the 2nd mode of vibration contributes only a 2% to the variance of the tip deflection and a 9% to the variance of the tip acceleration (Table 2).

As a first step, the case in which a TMD with a mass of 1% of the first modal mass of the structure, a damping ratio $\xi_{TMD} = 0.05$, tuned to the first natural frequency, was attached to the roof of the structure was considered (case 1a). The variance of the 1st mode resonant part of the tip deflection reduces to 27% of that of the plain structure, and the total rms tip deflection to 65%. In this case, the contribution of the second mode of vibration to the variance of the tip deflection is 4% and to the variance of the tip acceleration 26%.

A further slight reduction in the tip displacement can be obtained with a tuning of 96% of the first natural frequency of the structure (case 2a). In this case, the variance of the 1st mode resonant part of the tip deflection is reduced to 25% of that of the plain structure and the total rms tip deflection to 62%. The contributions of the second mode of vibration to the variance of the tip deflection and to the variance of the tip acceleration are almost the same as in previous case. The power spectral density functions of the tip deflection of the plain structure and of cases 1a and 2a are shown in Fig. 4, from which it appears that the second mode still contributes very little to the rms tip deflection.

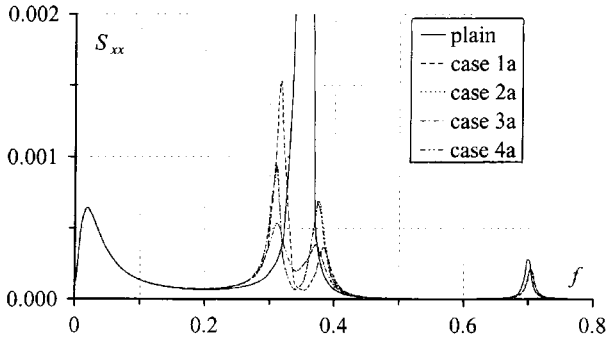

Fig. 4 Example 1 : PSDF of the tip displacement of the modified building

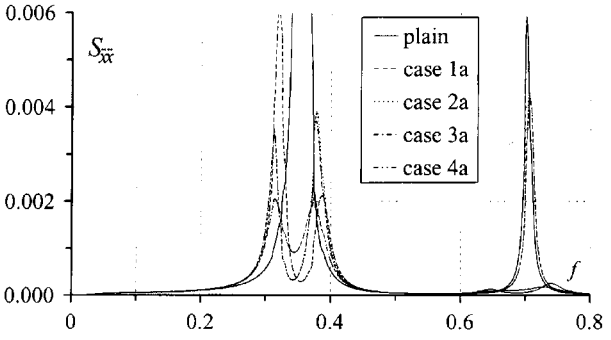

Fig. 5 Example 1 : PSDF of the tip acceleration of the modified building

A further reduction of the tip deflection can be achieved by optimising the damper's damping. However, it appears that if the concern is with the accelerations, a more consistent reduction of the response is obtained by reducing the response in the second mode (Fig. 5).

For this reason a second TMD, having the same mass and damping ratio of the first and tuned to 96% of the second natural frequency, was attached to the structure at midheight (case 3a). The reduction of the rms tip deflection with respect to case 2a is only 1%, however a 12% reduction appears in the rms tip acceleration (Table 2 and Fig. 5). The position of the second TMD was chosen based on the second mode shape. Mid-height corresponds to one of

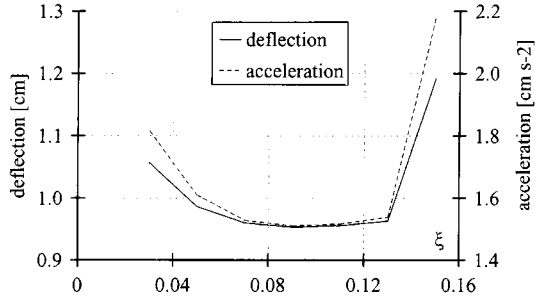

Fig. 6 Example 1 : Tip deflection and acceleration of the modified building as a function of the TMD damping

the two extremes of the mode shape (the other being at the tip of the structure), and a TMD tuned to the second mode proves to be more effective if placed at midheight rather than at the tip of the structure.

At this stage, one can try to improve the performance of the two TMDs by acting on their damping. Six more cases were analysed with different TMDs' damping ratios (the same damping ratio for the two TMDs). Damping ratios of 0.03, 0.07, 0.09, 0.11, 0.13 and 0.15 were considered. In Fig. 6, the rms tip deflection and acceleration are plotted as a function of the TMDs' damping ratio, showing how the best performance of the dampers can be obtained with a damping ratio of 0.09 (case 4a).

The final result is that reductions of 41% and 54% are achieved in the total rms tip deflection and acceleration respectively.

5.2. Example 2

A steel chimney 120 m tall, 8 m in diameter and with a mass of 1600 Kg/m was considered. The first mode natural frequency and damping ratio were $f_1 = 0.6$ Hz and $\xi_1 = 0.2\%$ respectively. The structure has cantilever mode shapes. The Strouhal number, spectral bandwidth and rms vortex shedding lift coefficient are $S = 0.20$, $B = 0.30$ and $\tilde{C}_{LS} = 0.20$ respectively (Vickery 1993). The exponent of the mean wind speed power law is 0.15, corresponding to open country, and the intensity of the longitudinal turbulence is $I_u = 0.10$.

Due to its low damping, the structure is prone to lock-in, and the rms tip displacement at resonance calculated using Eq. (27) is $\tilde{y} = 3.15$ m. The effectiveness of a TMD attached to the tip of the chimney in reducing the response was analysed. Two devices were considered: 1% (480 Kg) and 5% (2400 Kg) of the first modal mass of the chimney.

In Fig. 7a and 7b, the rms tip deflection is plotted as a function of the wind velocity for values of the tuning ratio of 1.00, 0.98 and 0.96 and for values of the damper's damping of 0.05 and 0.11. The wind velocity at which the maximum response occurs appears to be independent of the tuning and TMD damping, and only weakly dependent on the mass ratio ($U_{10} = 20$ m/s for $\mu = 0.01$ and $U_{10} = 19$ m/s for $\mu = 0.05$). In all the cases, the response is low enough to make the term $(\tilde{y}/\alpha)^2$ in Eq. (27) negligible, which validates the procedure.

In Figs. 8a and 8b, the rms TMD displacement is plotted as a function of the wind velocity.

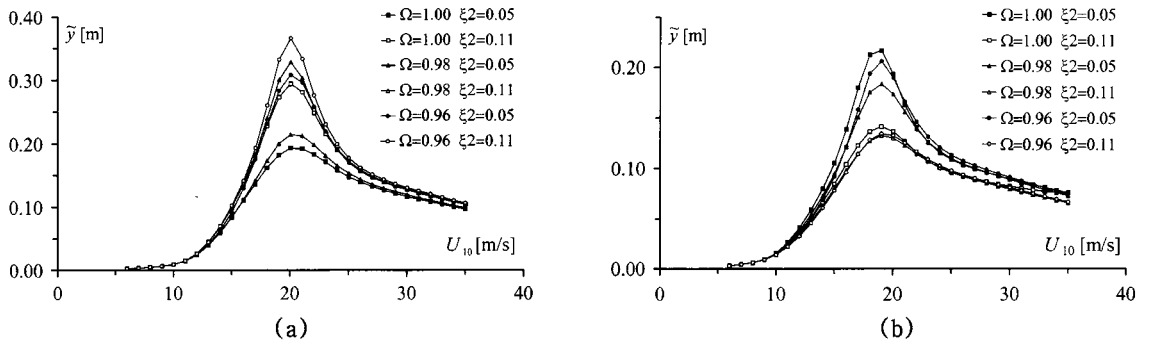

Fig. 7 a) Example 2 : Tip deflection as a function of the wind velocity for a mass ratio μ=0.01
b) Example 2 : Tip deflection as a function of the wind velocity for a mass ratio μ=0.05

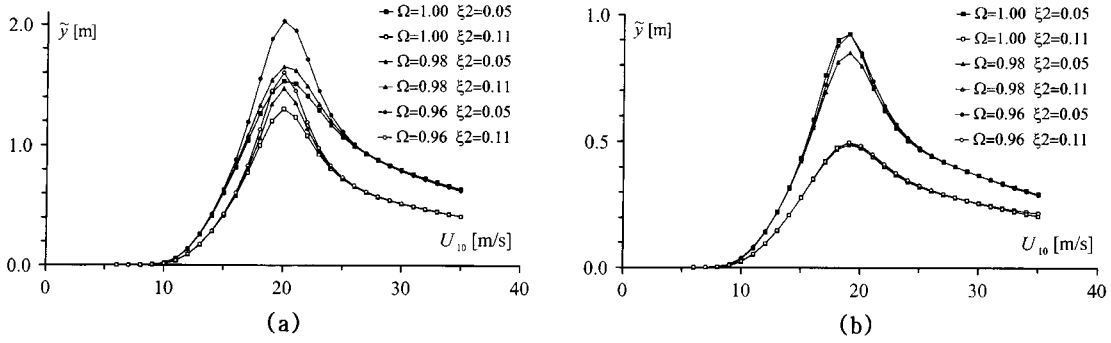

Fig. 8 a) Example 2 : TMD displacement as a function of the wind velocity for a mass ratio μ=0.01,
b) Example 2 : TMD displacement as a function of the wind velocity for a mass ratio μ=0.05

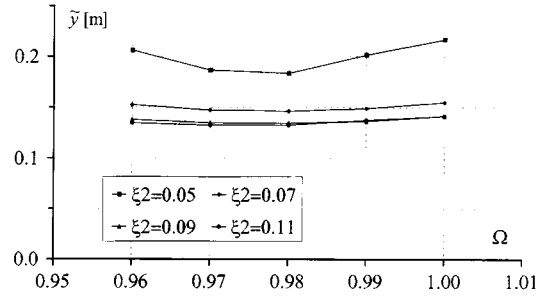

Fig. 9 Example 2 : Tip displacement for a mass ratio μ=0.05 and a wind velocity of 19 m/s

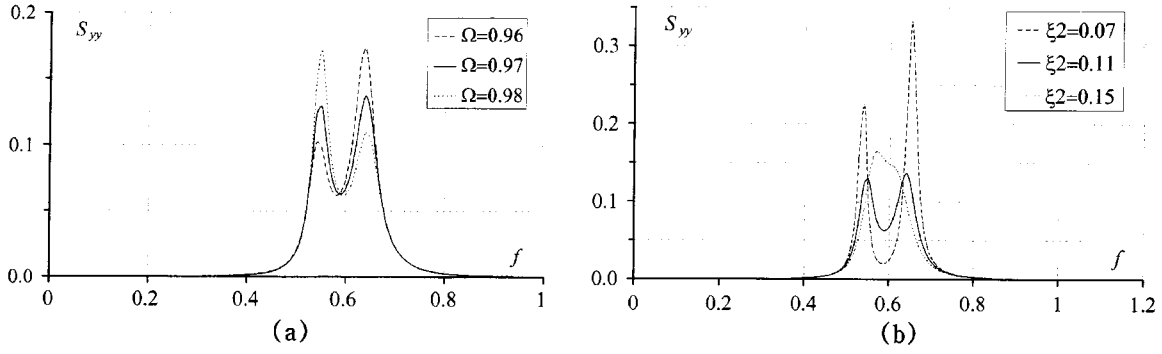

Fig. 10 a) Example 2 : PSDF of the tip displacement for a mass ratio μ=0.05, a wind velocity of 19 m/s and a damping $\xi_2 = 0.11$
b) Example 2 : PSDF of the tip displacement for a mass ratio μ=0.05, a wind velocity of 19 m/s and a tuning Ω=0.97

The curves show that the TMD has a maximum response at the same wind velocity at which the structure has its maximum response. As the mass ratio increases, the TMD response tends to be independent of tuning.

In Fig. 9, the rms tip deflection corresponding to a mass ratio $\mu = 0.05$ and a wind speed of 19 m/s is plotted as a function of the tuning ratio for different values of the damper's

damping. It appears that the best performance is obtained for a tuning of about $\Omega = 0.975$ and a damping $\xi_2 = 0.11$, in which case a rms tip displacement $\tilde{y} = 0.133$ m is calculated. Finally in Figs. 10a and 10b, the PSDF of the tip displacement is plotted for different TMD arrangements. The first plot shows the effect of a TMD mistuning on the system with optimum damping, while the second plot shows the effect of a TMD overdamping or underdamping the system with optimum tuning.

5.3. Example 3

As a third example, the galloping behaviour of a tall building was considered. The structure is a square building 252 m in height and 30 m in plan, with a mass per unit length of 2.25×10^5 kg/m. A drag coefficient $C_D = 1.4$ and a derivative of the lift coefficient $C'_L = -4.17$ were used for the square cross-section. The structure was considered in its first, cantilever mode of vibration, with a natural frequency of 0.2 Hz and a damping ratio of 0.8%, and a power law with an exponent $\alpha = 0.40$ was used for the mean wind speed profile. Critical wind speeds $U_{10c} = 25.4$ m/s and $U_{10c} = 25.2$ m/s were calculated using the procedure presented in this paper and the approach by Abdel-Rohman respectively, showing quite a good agreement between the results.

To increase the critical speed, a TMD is attached to the structure at the roof level. The added mass is 0.6% of the modal mass of the main structure while the tuning and the TMD

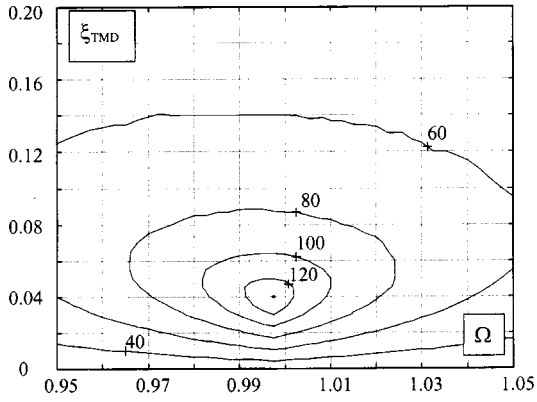

Fig. 11 Example 3 : Galloping wind speed as a function of tuning and TMD damping

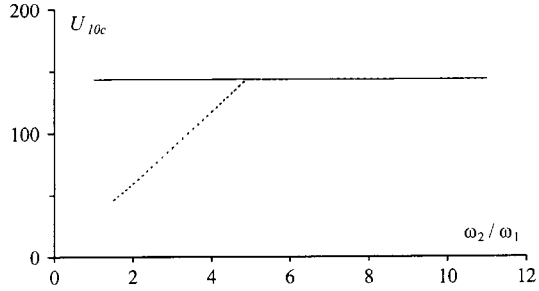

Fig. 12 Example 3 : Galloping wind speed as a function of ratio of the second to the first natural frequency

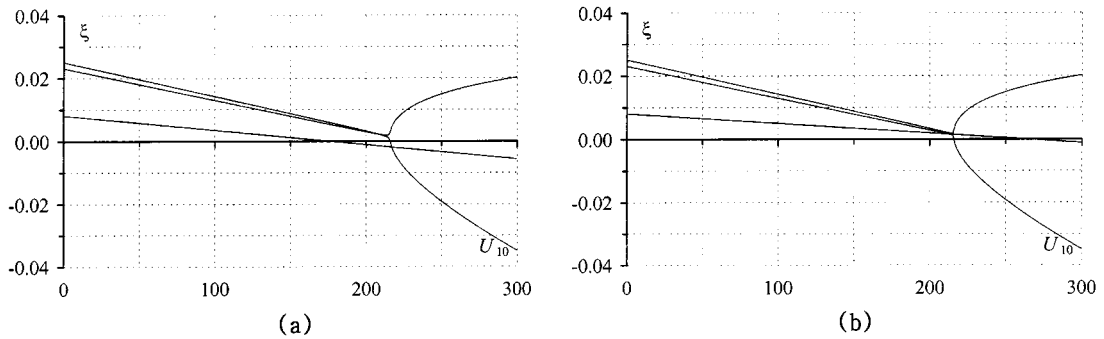

Fig. 13 a) Example 3 : Modal damping ratios as a function of wind speed for ω_2/ω_1=4
b) Example 3 : Modal damping ratios as a function of wind speed for ω_2/ω_1=6

damping were varied to study their influence on the performance of the device. In Fig. 11 the critical wind speed of the controlled structure is plotted as a function of tuning and damper's damping. It appears that the optimum tuning and damping ratio are $\Omega = 0.997$ and $\xi_{TMD} = 0.04$ respectively, leading to a critical wind speed $U_{10c} = 143.3$ m/s.

The effect of the TMD can be seen as an increase in the inherent damping of the plain primary system. In this case the effective damping was raised from 0.8% to 4.40%, 15% higher than the value derived following the approach by Fujino and co-workers (= 3.74%).

The second mode of vibration of the primary system was at this point introduced in the calculations. In Fig. 12, the critical speed is plotted as a function of the ratio between the second and first natural frequencies of the primary system. The second mode of vibration of the structure is the second cantilever mode, with a damping of 0.8% of critical and the TMD parameters are the optimum values calculated on the single mode structure. It can be seen that for values of the ratio between the two frequencies of 4.9 or more the first mode of vibration dominates the galloping behaviour and the critical speed is almost coincident with that calculated by accounting for only one mode of vibration (straight line in the plot). However for $\omega_2 / \omega_1 < 4.9$, galloping in the second mode occurs at a wind speed lower than the first mode critical speed. The behaviour can be understood from Figs. 13a and 13b, where the total modal damping ratios (structural + aerodynamic) are plotted as a function of the wind speed for $\omega_2/\omega_1 = 4$ and $\omega_2/\omega_1 = 6$, showing the changes in the second mode damping occurring with varying frequency.

6. Conclusions

Due to their well established effectiveness in reducing the response of dynamic systems, Tuned Mass Dampers have found, in the last nine decades, a wide range of applications in different fields of engineering. Their intuitive behaviour led to simplified models to analyse their performance, and closed form expression for the optimum TMD parameters as well as for the system response were found for many practical cases. The simplifying assumptions, however, make the models available in the literature not suitable for the analysis of more general cases. In civil engineering applications, in fact, it is often necessary to account for coupled modes of vibration, to consider the possibility of using more than one TMD, to optimise the number,

position and characteristics of the TMDs with respect to any parameter of the structural response and to account for realistic spectra of the excitation. A procedure that accounts for all the above features and bringing to closed form expressions, though, seems unrealistic.

In the present paper, a mathematical linear model, that relies on numerical calculations, for the analysis of complicated structures, including all the above features, was presented. The model calculates the PSDF of any response parameter, accounting for an arbitrary number of structural modes of vibration, an arbitrary number of TMDs and an arbitrary excitation.

The model analyses the stability of the system and calculates its steady state response and is thus suitable for the analysis of structures subjected to wind action. Three examples were presented in which the procedure was applied to the evaluation of the buffeting response and galloping behaviour of two tall buildings, and to the evaluation of the vortex shedding induced response of a steel chimney.

In the case of the tall building subjected to buffeting, it was found that the optimum tuning and damper's damping calculated by accounting for a real turbulence spectrum are respectively lower and higher than the corresponding values found with a white noise input. Moreover it was found that a second TMD tuned to the second natural frequency of the structure may be effective if the structural accelerations are of concern.

In the case of the vortex shedding induced response of a chimney, it was found that an added mass as low as 1% of the first modal mass of the structure is enough to prevent lock-in and to keep the structural response within acceptable limits.

For the tall building subject to galloping, the optimum TMD parameters were found that maximise the critical speed. In general it was found that if the first mode is controlled by a TMD and if the second natural frequency is not much higher than the first, galloping in the second mode may occur at a wind velocity lower than the first critical.

Acknowledgements

The author wishes to express his gratitude to Prof. Giovanni Solari, whose encouragement and advice were essential to this work.

References

Abdel-Rohman M. (1994), "Design of tuned mass dampers for suppression of galloping in tall prismatic structures", *J. Sound Vib.*, **171**(3), 289-299.

Ayorinde E.O. and Warburton G.B. (1980), "Minimising structural vibrations with absorbers", *Earthquake Engng. Struct. Dyn.*, **8**, 219-236.

Bapat V.A. and Kumaraswamy H.V. (1979), "Effect of primary system damping on the optimum design of an untuned viscous dynamic vibration absorber", *J. Sound Vib.*, **63**, 469-474.

Borino G. and Muscolino G. (1986), "Mode superposition methods in dynamic analysis of classically and non-classically damped linear systems", *Earthquake Engng. Struct. Dyn.*, **14**, 705-717.

Brock J.E. (1946), "A note on the damped vibration absorber", *J. Appl. Mech. ASME*, **13**, A-284.

Crandall S.H. and Mark W.D. (1963), *Random Vibration in Mechanical Systems*, Academic Press, New York.

Curtis J.A. and Boykin T.R. (1961), "Response of two-degree-of freedom systems to white noise base excitation", *J. Acoust. Soc. Amer.*, **33**, 655-663.

Den Hartog J.P. (1940), *Mechanical Vibrations*, McGraw-Hill, New York.

Falcon K.C., Stone B.J., Simcock W.D. and Andrew C. (1967), "Optimisation of vibration absorbers: a graphical method for use on idealised systems with restricted damping", *J. Mech. Engng. Sci.*, **9**, 374-381.

Fujino Y., Warnitchai P. and Ito M. (1985), "Suppression of galloping of bridge tower using tuned mass damper", *J. Fac. Engng. U. of Tokyo*, **38**, 49-73.

Gupta Y.P. and Chandrasekaran A.R. (1969), "Absorber system for earthquake excitation", *Proc. 4th World Conf. Earthquake Engng.*, Santiago, Chile.

Jacquot R.G. and Hoppe D.L. (1973), "Optimal random vibration absorbers", *J. Engng. Mech. ASCE*, **99**, 612-621.

Jacquot R.G. (1978), "Optimal dynamic vibration absorbers for general beam systems", *J. Sound Vib.*, **60**, 535-542.

Kaynia A.M., Veneziano D. and Biggs J. (1981) "Seismic effectiveness of tuned mass dampers", *J. Struct. Eng. ASCE*, **107**, 1465-1484.

Luft R.W. (1979), "Optimal tuned mass dampers for buildings", *J. Struct. Engng. ASCE*, **105**, 2766-2772.

McNamara R.J. (1977), "Tuned mass dampers for buildings", *J. Struct. Engng. ASCE*, **103**, 1785-1798.

Neubert V.H. (1964), "Dynamic absorbers applied to a bar that has solid damping", *J. Acoust. Soc. Amer.*, **36**, 673-670.

Occhiuzzi A. and Ricciardelli F. (1996), "L'effetto degli smorzatori a massa accordata sulla risposta delle strutture allungate all'azione del vento", *Proc. 4th Italian Nat. Conf. Wind Engng.*, Trieste.

Ormondroyd J. and Den Hartog J.P. (1928), "The theory of the dynamic vibration absorber", *J. Appl. Mech. ASME*, 50.

Ricciardelli F. (1996), "Risposta delle torri di ponti di grande luce all'azione del vento", Ph.D. thesis, Universita` di Napoli Federico II, Napoli, Italy.

Samali B., Yang J.N., Yeh C.T. (1985), "Control of the lateral-torsional motion of wind-excited buildings", *J. Engng, Mech. ASCE*, **111**, 777-796.

Sladek J.R. and Klinger R.E. (1983), "Effect of tuned mass damper on seismic response", *J. Struct. Engng. ASCE*, **109**, 2004-2009.

Snowdon J.C. (1959), "Steady-state behaviour of the dynamic absorber", *J. Acoust. Soc. Amer.*, **31**, 1096-1103.

Snowdon J.C. (1966), "Vibration of cantilevers to which dynamic absorbers are attached", *J. Acoust. Soc. Amer.*, **39**, 878-886.

Solari G. (1994), "Gust excited-vibrations" *Wind-excited Vibrations of Structures* H. Sockel ed., Springer-Verlag.

Srinivasan A.V. (1969), "Analysis of parallel damped dynamic vibration absorbers", *J. of Engng. for Industry ASME*, **91**, 282-287.

Tsai H.C. and Lin G.C. (1993), "Optimum tuned-mass dampers for minimizing the steady-state response of support-excited and damped systems", *Earthquake Engng. Struct. Dyn.*, **22**, 957-973.

Vickery B.J. (1993), "Across-wind loading on reinforced concrete chimneys of circular cross-section", BLWT-4-1993, The Boundary Layer Wind Tunnel Laboratory, Faculty of Engineering Science, The University of Western Ontario, London, Canada.

Warburton G.B. and Ayorinde E.O. (1980), "Optimum absorber parameters for simple systems", *Earthquake Engng. Struct. Dyn.*, **8**, 197-217.

Wirsching P.H. and Campbell G.W. (1974), "Minimal structural response under random excitation using the vibration absorber", *Earthquake Engng. Struct. Dyn.*, **2**, 303-312.

Xu Y.L., Kwok K.C.S. and Samali B. (1992a), "Control of wind-induced tall building vibration by tuned mass dampers," *J. Wind Engng. Ind. Aero.*, **40**, 1-32.

Xu Y.L., Kwok K.C.S. and Samali B. (1992b), "The effect of tuned mass dampers and liquid dampers on cross-wind response of tall/slender structures", *J. Wind Engng. Ind. Aero.*, **40**, 33-54.

(*Communicated by Giovanni Solari*)